ORIGINAL ARTICLE

Lung Endothelial MicroRNA-1 Regulates Tumor Growth and Angiogenesis

Asawari Korde[1]*, Lei Jin[1,2]*, Jian-ge Zhang[3], Anuradha Ramaswamy[1], Buqu Hu[1], Saeed Kolahian[4], Brenda Juan Guardela[1], Jose Herazo-Maya[1], Jill M. Siegfried[5], Laura Stabile[6], Margaret A. Pisani[1], Roy S. Herbst[7], Naftali Kaminski[1], Jack A. Elias[8], Jonathan T. Puchalski[1], and Shervin S. Takyar[1]

[1]Section of Pulmonary, Critical Care, and Sleep Medicine and [7]Yale Comprehensive Cancer Center, Yale University School of Medicine, New Haven, Connecticut; [2]Cleveland Clinic Cole Eye Institute and Lerner Research Institute, Cleveland, Ohio; [3]Department of Medicinal Chemistry, School of Pharmaceutical Science, Zhengzhou University, Zhengzhou, Henan, China; [4]Department of Pharmacology and Experimental Therapy, University of Tübingen, Tübingen, Germany; [5]Department of Pharmacology, Masonic Cancer Center, University of Minnesota Medical School, Minneapolis, Minnesota; [6]Department of Pharmacology and Chemical Biology, University of Pittsburgh Cancer Institute, Hillman Cancer Center, Pittsburgh, Pennsylvania; and [8]Division of Biology and Medicine, Warren Alpert School of Medicine at Brown University, Providence, Rhode Island

Abstract

Rationale: Vascular endothelial growth factor down-regulates microRNA-1 (miR-1) in the lung endothelium, and endothelial cells play a critical role in tumor progression and angiogenesis.

Objectives: To examine the clinical significance of miR-1 in non–small cell lung cancer (NSCLC) and its specific role in tumor endothelium.

Methods: miR-1 levels were measured by Taqman assay. Endothelial cells were isolated by magnetic sorting. We used vascular endothelial cadherin promoter to create a vascular-specific miR-1 lentiviral vector and an inducible transgenic mouse. $KRAS^{G12D\ mut}/Trp^{53-/-}$ (KP) mice, lung-specific vascular endothelial growth factor transgenic mice, Lewis lung carcinoma xenografts, and primary endothelial cells were used to test the effects of miR-1.

Measurements and Main Results: In two cohorts of patients with NSCLC, miR-1 levels were lower in tumors than the cancer-free tissue. Tumor miR-1 levels correlated with the overall survival of patients with NSCLC. miR-1 levels were also lower in endothelial cells isolated from NSCLC tumors and tumor-bearing lungs of KP mouse model. We examined the significance of lower miR-1 levels by testing the effects of vascular-specific miR-1 overexpression. Vector-mediated delivery or transgenic overexpression of miR-1 in endothelial cells decreased tumor burden in KP mice, reduced the growth and vascularity of Lewis lung carcinoma xenografts, and decreased tracheal angiogenesis in vascular endothelial growth factor transgenic mice. In endothelial cells, miR-1 level was regulated through phosphoinositide 3-kinase and specifically controlled proliferation, *de novo* DNA synthesis, and ERK1/2 activation. Myeloproliferative leukemia oncogene was targeted by miR-1 in the lung endothelium and regulated tumor growth and angiogenesis.

Conclusions: Endothelial miR-1 is down-regulated in NSCLC tumors and controls tumor progression and angiogenesis.

Keywords: microRNA-1; angiogenesis; lung cancer; tumor microenvironment; vascular endothelial growth factor blockers

(Received in original form October 28, 2016; accepted in final form August 28, 2017)

*These authors contributed equally to this work.

Supported by the NHLBI (K99/R00) and the American Lung Association Lung Cancer Discovery Award.

Author Contributions: L.J., A.K., J.-g.Z., and S.K., experimental work. A.K. took part in writing and formatting the manuscript. A.R., clinical data collection and analysis. B.H., data analysis. B.J.G. and J.H.-M., collection and processing of clinical samples and data analysis. J.M.S. and L.S., collection of clinical samples. M.A.P., design of the clinical study. R.S.H., study conception and design. N.K., review of the manuscript. J.A.E., conception and design of VEGF transgenic studies. J.T.P. and A.R., collection and processing of clinical samples. S.S.T., study conception and design, experimental work, and writing and editing of the manuscript.

Correspondence and requests for reprints should be addressed to Shervin S. Takyar, M.D., Ph.D., 300 Cedar Street, New Haven, CT 06519. E-mail: seyedtaghi.takyar@yale.edu

This article has an online supplement, which is accessible from this issue's table of contents at www.atsjournals.org

Am J Respir Crit Care Med Vol 196, Iss 11, pp 1443–1455, Dec 1, 2017

Originally Published in Press as DOI: 10.1164/rccm.201610-2157OC on August 30, 2017
Internet address: www.atsjournals.org

At a Glance Summary

Scientific Knowledge on the Subject: Tumor endothelial cells are integral components of the tumor microenvironment, and angiogenesis is a hallmark of tumor progression. However, current antiangiogenic therapies have limited clinical efficacy. MicroRNAs regulate various cellular responses and are prime targets for antitumor therapies. The specific role of microRNAs in the tumor endothelium has not been adequately studied.

What This Study Adds to the Field: MicroRNA-1 is down-regulated in the non–small cell cancer tumor endothelium, and tumor microRNA-1 levels correlate with overall survival of patients with lung adenocarcinoma. MicroRNA-1 is also down-regulated in the endothelium of lung adenocarcinoma models and regulates tumor progression, endothelial proliferation, and extracellular signal–regulated protein kinases 1/2 signaling.

Endothelial cells are critical components of the tumor microenvironment, and tumor vascularity closely correlates with tumor progression and invasiveness (1–3). Vascular endothelial growth factor (VEGF) is one of the main orchestrators of tumor angiogenesis, and anti-VEGF agents are currently approved for the treatment of advanced lung cancer (4).

MicroRNAs (miRNAs) are small (21–24 nt) RNAs that regulate gene expression by base pairing with specific sequences within messenger RNAs (5–10). miRNAs are altered in malignancies and in many instances impart a significant effect on tumor behavior (11, 12). We had previously shown that VEGF regulates miRNA-1 (miR-1) levels in the lung endothelium of asthma models (13). Regarding the importance of VEGF in tumor progression and angiogenesis, we sought to determine the role of miR-1 in non–small cell lung cancer (NSCLC) tumors.

We found that miR-1 levels in NSCLC tumors are lower than the adjacent cancer-free tissues and correlate inversely with overall survival. miR-1 was also lower in the endothelial cells isolated from these tumors and was down-regulated in the lung endothelium of the Kirsten rat sarcoma viral oncogene homolog (*KRAS*) mutant/transformation-related protein 53 (*P53* or *Trp53*) knockout (KP) mouse model of NSCLC on tumor formation. Vascular-specific overexpression of miR-1 significantly decreased tumor burden in NSCLC models and reduced tumor and lung angiogenesis.

Methods

NSCLC Patient Sample Preparation

The early–late NSCLC (all-NSCLC) cohort consisted of 68 patients with NSCLC who underwent surgical resection (n = 34) or bronchoscopy (n = 34) (*see* Table E1 in the online supplement) at the Yale Cancer Center. The early lung adenocarcinoma (early LA) cohort consisted of 41 patients who underwent surgical resection (n = 41) (*see* Table E2) at the University of Pittsburgh Medical Center. Research design, procedures, and human subject approvals are described in the online supplement.

miRNA and Messenger RNA Analysis by Quantitative Real-Time Polymerase Chain Reaction

miRNAs and messenger RNAs were measured using Taqman assays (Life Technologies, Carlsbad, CA) and SYBR green quantitative real-time polymerase chain reaction (Biorad, Hercules, CA) and

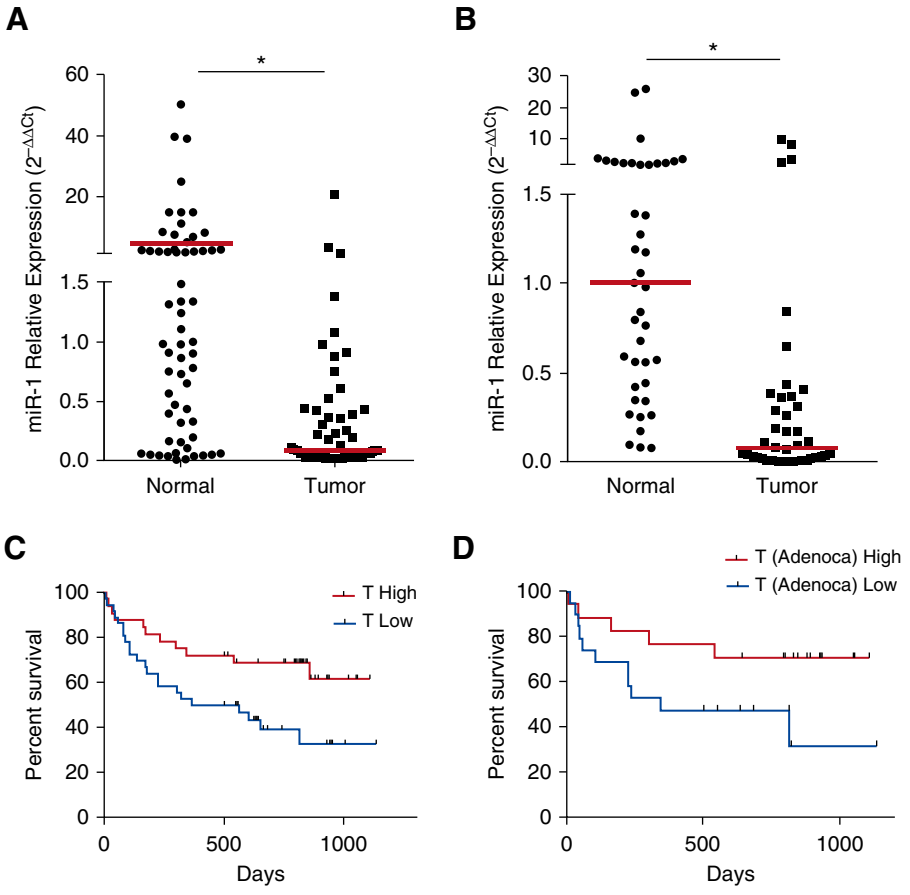

Figure 1. The clinical significance of microRNA-1 (miR-1) levels in non–small cell lung cancer. (*A*) Mature miR-1/18s (control gene) levels were measured in tumors and cancer-free lung tissue samples from the all–non–small cell lung cancer cohort. Values were normalized to the median of the normal samples and expressed as $2^{-\Delta\Delta Ct}$ ($n_{Tumor} = 61$, $n_{Normal} = 57$; $^*P = 0.0033$). (*B*) miR-1 values in samples from the early lung adenocarcinoma cohort were measured and graphed as in *A* ($n_{Tumor} = 41$, $n_{Normal} = 41$; $^*P < 0.0001$). In *A* and *B*, *red bars* show medians in each group. (*C*) Patients were divided into T-high and T-low groups based on the median of all tumor miR-1 levels in the cohort. Kaplan-Meier graph shows survival (in days) for T-high and T-low patients (n = 61; $P = 0.0082$). (*D*) Patients with lung adenocarcinoma (Adenoca) were divided into T-high and T-low groups and their survival compared as described in *C* (n = 36; $P = 0.0189$). In *C* and *D*, *gray tick marks* indicate censored patients.

according to the manufacturer's instructions (13).

Isolation of Endothelial Cells from Murine Lung by Magnetic-activated Cell Sorting

Endothelial ($CD31^+$, $CD45^-$, or $CD105^+$, $CD45^-$) and hematopoietic ($CD45^+$) cells were isolated using Miltenyi Biotech (Auburn, CA) magnetic columns as described previously (13).

Mice Used in the Study

Animal protocols were approved by the Yale University Institutional Animal Care and Use Committee. CC10-reverse tetracycline-controlled transactivator (rtTA)-VEGF transgenic mice and measurement of tracheal angiogenesis have been described previously (14) and in the online supplement. Generation of miR-1 transgenic mice is described in the online supplement. In the Lewis lung carcinoma (LLC) model, 2×10^6 tumor cells were implanted subcutaneously, and the size of the implants was monitored. When the tumor sizes reached 5–10 mm in diameter, they were injected with vectors and controls, and their sizes were monitored every other day over the next 10 days. The maintenance, use, and cross-breeding of $Kras^{LSL\text{-}G12D}/Trp53^{flx/flx}$ mouse (KP mouse) are described in the online supplement.

Cell Culture

Mouse lung endothelial cells (MLECs) were isolated from murine lungs as described previously (13). Human umbilical vein endothelial cells (HUVECs) were purchased from the Department of Vascular Biology and Therapeutics Program at Yale. Detailed descriptions of cell culture assays are described in the online supplement.

Short Hairpin RNA and Lentiviral Vectors

Vascular-specific miR-1 (V-miR-1) was generated by cloning vascular endothelial cadherin (VE-cadherin) promoter into pSIH-H1-copGFP Lentiviral vector (SBI, Palo Alto, CA) as described in the online supplement.

Statistical Analysis and Data Availability

A detailed description of statistical analysis is included in the online supplement. All relevant data are available from authors with restrictions for the human data.

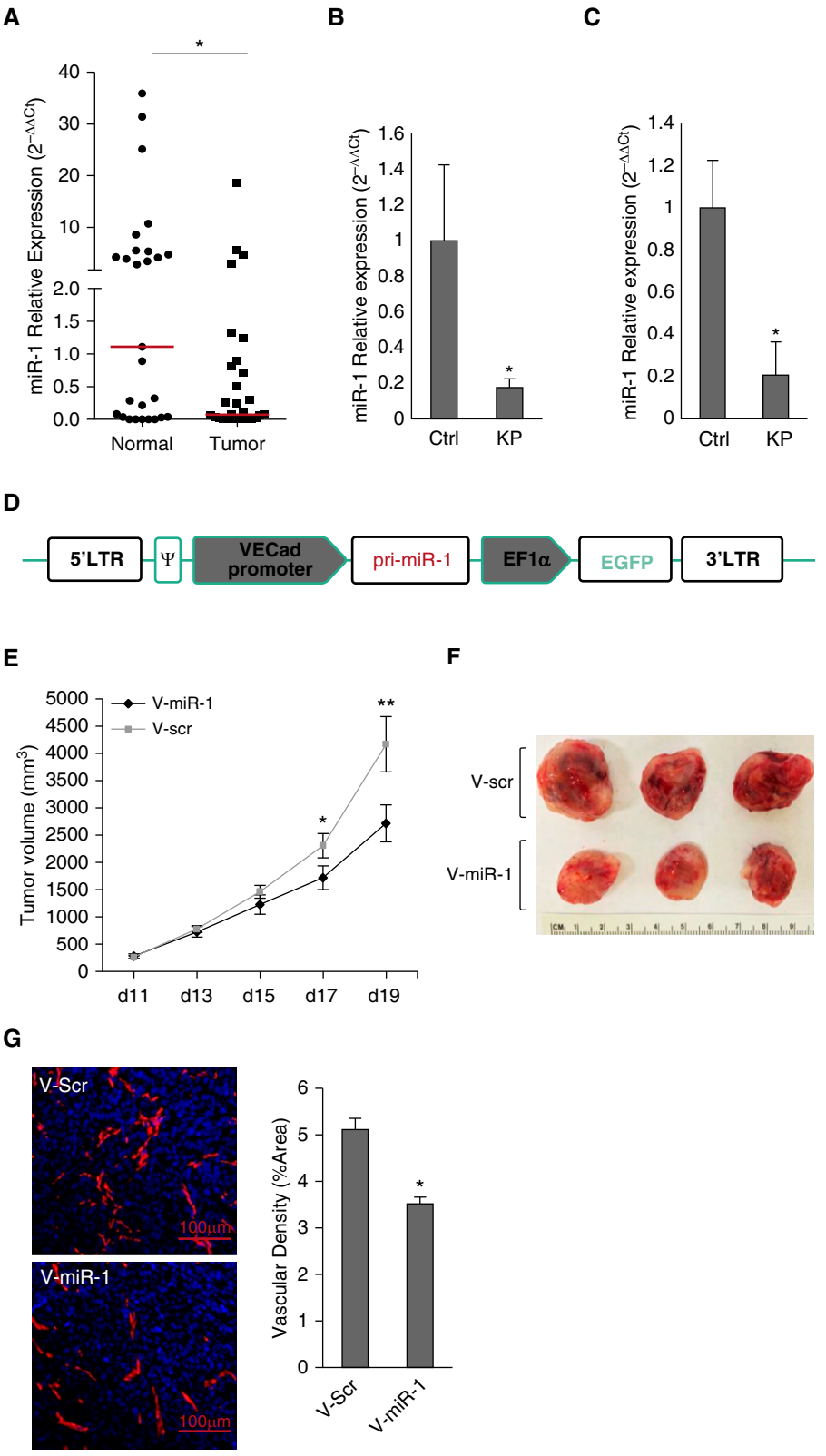

Figure 2. MicroRNA-1 (miR-1) is down-regulated in tumor endothelium and regulates angiogenesis. (*A*) Endothelial cells ($CD31^+$, $CD45^-$) were isolated from non–small cell lung cancer tumors (Tumor) and adjacent cancer-free tissues (Normal). miR-1/18s levels were normalized to the median of the control (Normal) group and expressed as $2^{-\Delta\Delta Ct}$ (n = 28; *$P = 0.0351$). *Red horizontal lines*

Results

miR-1 Level Is Lower in NSCLC Tumors and Correlates with Overall Survival

We examined the levels of mature miR-1 in tumor and cancer-free (normal) biopsy samples from a 68-patient cohort with early and late-stage NSCLC (all-NSCLC; *see* Table E1) and found that miR-1 levels were significantly lower in the tumor samples in the whole group (Figure 1A) and within both adenocarcinoma and squamous cell carcinoma subtypes (*see* Figures E1A and E1B). miR-1 levels were also lower than cancer-free tissue in a 41-patient cohort of early-stage lung adenocarcinoma (early LA; Figure 1B; *see* Table E2).

We next tested the clinical correlations of miR-1. In the all-NSCLC cohort, tumor miR-1 levels had a significant correlation with overall survival ($P = 0.0022$) and histologic subtype ($P = 0.0008$) and showed a strong trend toward lower levels in more advanced clinical stages ($P = 0.0708$), but no significant associations with age, sex, or tumor size (*see* Table E3A). In a subgroup analysis, miR-1 correlation with survival was only observed in the adenocarcinoma group (*see* Table E3B). Because of inadequate data and the short duration of follow-up, overall survival could not be assessed for the early-LA cohort.

High miR-1 Levels Predicted Longer Overall Survival

We next examined the value of tumor miR-1 levels as a predictor of tumor progression. The all-NSCLC cohort was divided into high miR-1 level (T-high) and low miR-1 level (T-low) groups based on the median of miR-1 levels within the cohort. T-high patients survived significantly longer than T-low patients ($P = 0.031$; *see* Table E3C) but showed no difference in sex, age, size of the tumor, or clinical stage. There was also a significant difference in the distribution of tumor histologic subtypes between the T-high and T-low patients ($P = 0.0018$). In Kaplan-Meier analysis, high miR-1 levels (T-high status) was predictive of longer survival (Figure 1C). Among tumor subtypes, miR-1 maintained this predictive ability only in the adenocarcinoma subgroup (Figure 1D). High miR-1 levels were also predictive of longer survival in a publicly available 542-patient lung adenocarcinoma cohort (The Cancer Genome Atlas Lung Adenocarcinoma; $P = 0.000487$; hazard ratio, 0.91 [0.86–0.96]) (*see* Figure E2).

miR-1 Is Down-regulated in the Tumor Endothelium

miR-1 levels were significantly lower in the endothelial ($CD45^-$, $CD31^+$) cells isolated from NSCLC tumors compared with their adjacent cancer-free tissues (Figure 2A), suggesting that the lower levels of miR-1 in the whole tumors are at least partly caused by its down-regulation in the endothelial compartment. We tested this hypothesis in the KP mouse model. Activation of floxed $Kras^{LSL\text{-}G12D}$ and deletion of $Trp53^{flx/flx}$ alleles in this model lead to tumor formation in 4–6 months (15). Mature miR-1 levels were more than 80% lower in the tumor-bearing lungs and endothelial cells isolated from these lungs, compared with the control subjects (Figures 2B and 2C).

Endothelial miR-1 Controls Tumor Growth and Vascularity

Lentiviral delivery model. To examine the importance of miR-1 down-regulation, we tested the effects of endothelial-specific miR-1 overexpression on tumor formation. We first constructed a vascular-specific lentiviral vector (V-miR-1) that contained VE-cadherin promoter (vascular-specific promoter) upstream from primary miR-1 (pri-miR-1) sequence, and eukaryotic elongation factor alpha (EF1α) promoter (a universal promoter driving expression in all cell types) (17) upstream from green fluorescent protein (Figure 2D). As expected (16, 17), V-miR-1 delivery led to green fluorescent protein expression in all lung structural cells (*see* Figure E3A), whereas miR-1 was only overexpressed in the lung endothelium (*see* Figures E3B–E3E). Delivery of V-miR-1 to fully formed LLC xenografts (250–500 mm^3 tumor volume) significantly decreased their growth rate and vascularity, showing the inhibitory effect of endothelial miR-1 in advanced tumors (Figures 2E–2G).

Transgenic model. We created an inducible vascular-specific miR-1 transgenic mouse model (miR-1 TG) by cloning miR-1 primary transcript (pri-miR-1) sequence downstream from a tetracycline-inducible cytomegalovirus promoter (tet-O-pCMV-pri-miR-1-hGH) and coexpressing this vector with a second construct containing VE-cadherin–driven transactivator (Figure 3A). Addition of doxycycline to the drinking water of these mice led to overexpression of miR-1 specifically in endothelium (Figure 3B). As with our lentiviral method, induction of miR-1 in this model also reduced the growth and vascularity of the fully formed (500 mm^3 tumor volume) LLC xenografts (Figures 3C and 3D).

Endothelial miR-1 Inhibits Tumor Growth in the KP Model

We next tested the role of endothelial miR-1 in the KP model. We created a

Figure 2. (Continued). indicate medians of the groups. (*B*) Kirsten rat sarcoma viral oncogene homolog (*KRAS*) mutant/transformation-related protein 53 (*P53*) (KP) knockout mice received intranasal Cre recombinase (or control [ctrl]) vector and their lungs harvested after 6 months. miR-1/18s levels were measured in the whole lungs, normalized to the mean of the control group, and expressed as $2^{-\Delta\Delta Ct}$ (n = 12 in each group from two experiments; $^*P = 0.01533$). (*C*) Endothelial ($CD31^+$, $CD45^-$) cells were isolated from the lungs of KP and ctrl mice and miR-1 levels were measured and normalized as described in *B* (n ⩾ 5 in each group from two experiments; $^*P = 0.016$). (*D*) Vascular-specific miR-1 expression vector (V-miR-1). Vascular endothelial cadherin (VECad) promoter was cloned upstream of primary (pri)-miR-1 sequence in a lentiviral transfer vector containing enhanced green fluorescent protein as a marker gene driven by elongation factor 1 α subunit (EF1α) promoter. (*E–G*) Effect of vascular-specific miR-1 overexpression on tumor growth and angiogenesis. Lewis lung carcinoma implants were injected with V-miR-1 or scrambled control vector (V-scr) on Day 10, and harvested on Day 19 after implantation. The sizes of the tumors were measured and volumes calculated according to the following formula: volume = 0.52 × $width^2$ × length. (*E*) Tumor volumes are graphed versus the time of measurement (number of days on the *x-axis*; data points are means of tumor volume) (n ⩾ 13 in each group from three experiments; $^*P = 0.036013$, $^{**}P = 0.016034$). (*F*) Representative tumors from the two groups on Day 19 after implantation. (*G*) Tumor sections were stained with anti-CD31 antibody and DAPI (4',6-diamidino-2-phenylindole). (*Left*) Representative images. (*Right*) Quantification of vessel density based on the percentage of CD31-positive areas/whole area examined (n ⩾ 7 in each group from two experiments; $^*P = 0.002645$). *Error bars* represent SEM. ψ = packaging signal; EGFP = enhanced green fluorescent protein; LTR = long terminal repeat.

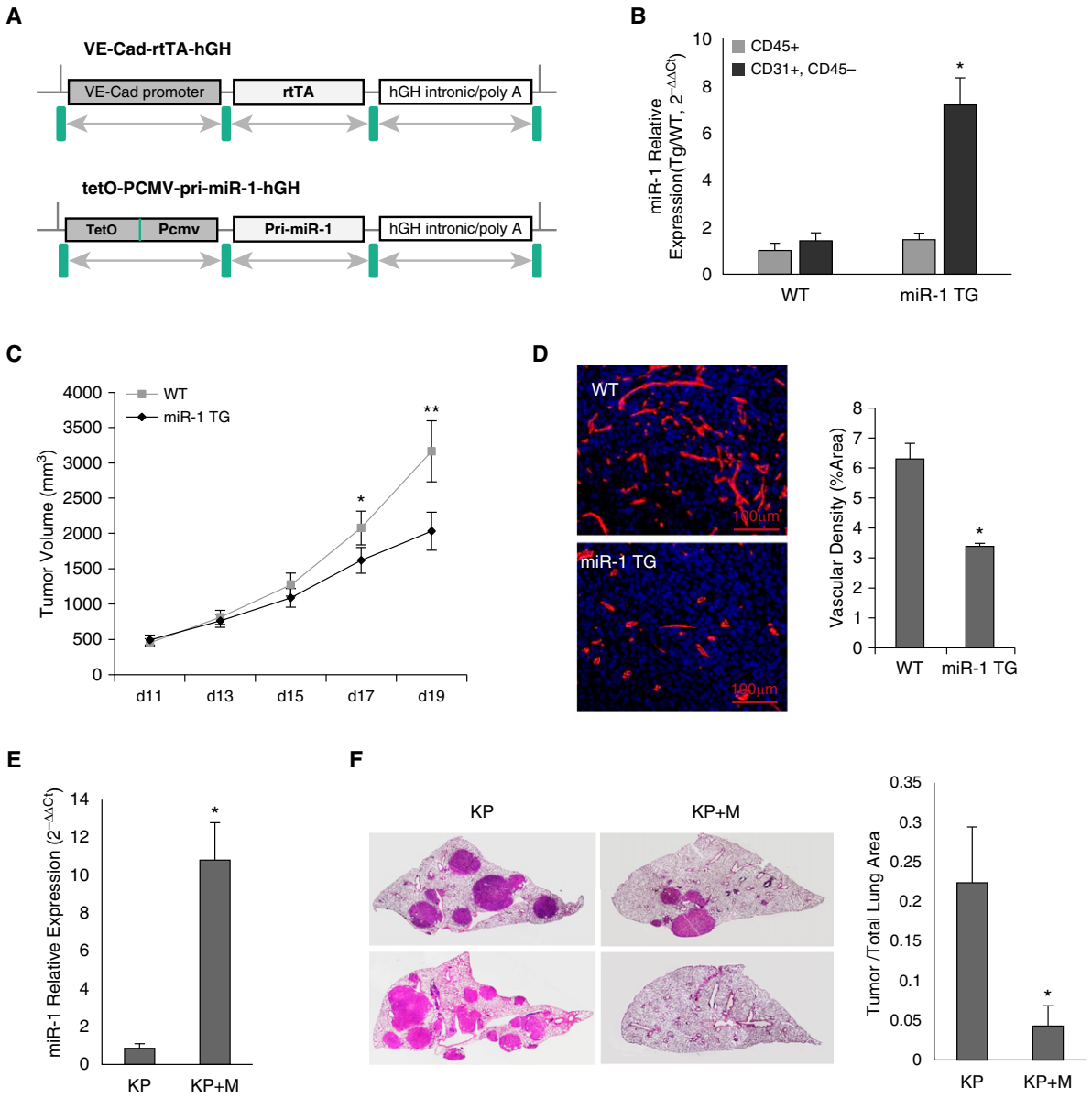

Figure 3. The effects of vascular-specific microRNA-1 (miR-1) in the transgenic model. (*A*) Constructs used for the generation of inducible endothelial-specific transgenic mouse. VE-Cad-rtTA-hGH: contains vascular endothelial cadherin (VE-Cad) promoter, reverse tetracycline transactivator (rtTA), and human growth hormone (hGH) intronic, nuclear localization, and polyadenylation sequences. tet-O-pCMV-pri-miR-1-hGH: contains a polymeric tetracycline operator (tet-O), minimal cytomegalovirus (CMV) promoter, and hGH intronic, polyadenylation, and nuclear localization signals flanking its multiple cloning site. Primary (pri)-miR-1 sequence was cloned between the hGH intronic sequence and tet-O-CMV promoter. (*B*) miR-1 levels were measured in endothelial ($CD31^+$, $CD45^-$) and immune ($CD45^+$) cell fractions isolated from wild-type and miR-1 transgenic (miR-1 TG) mice. *Bar graphs* represent mean level of miR-1 expressed as $2^{-\Delta\Delta Ct}$ value (*see* supplementary methods for description of normalization). The *asterisk* indicates significant increase in $CD31^+$ $CD45^-$ fraction as compared to $CD45^+$ fraction in the miR-1 TG group (n = 4 per group; $^*P = 0.001768$). (*C* and *D*) The effects of miR-1 transgene expression on tumor growth and angiogenesis in Lewis lung carcinoma model. Tumor implantation and volume measurements performed as described in Figure 2E (n ⩾ 4 from three experiments; $^*P = 0.033645$; $^{**}P = 0.007521$). (*D*) Tumors sections were stained with anti-CD31 antibody and analyzed for vascular density as described in Figure 2G. (*Left*) Representative images of tumors. (*Right*) Quantification of CD31-positive area (vascular density) expressed as percentage of the whole area examined (n ⩾ 12 from three experiments; $^*P = 0.017903$). (*E* and *F*) The effect of endothelial miR-1 in Kirsten rat sarcoma viral oncogene homolog (*KRAS*)/transformation-related protein 53 (*P53*) knockout (KP) model. KP and KP + M mice (KP cross with miR-1-TG mice) received Cre recombinase at 1 month of age. miR-1 overexpression was induced by adding doxycycline to the drinking water 5 months after Cre delivery and lungs were harvested 6 months after Cre delivery. (*E*) Relative expression of miR-1 (miR-1/18s in KP + M and KP mice normalized to the levels in KP mice) in endothelial cells isolated from these lungs (n = 9 from 2 experiments; $^*P = 0.001211$). (*F*) Lungs were sectioned (5 μm) and stained with hematoxylin and eosin. Tumor burden was determined by measuring tumor area/whole lung area. (*Left*) Representative images of the lungs from two mice in each group (each image was assembled from multiple smaller images at ×400 magnification). (*Right*) Quantification of tumor burden in the two groups (n = 9 from two experiments; $^*P = 0.02887$). *Error bars* represent SEM. WT = wild-type.

quadruple-transgenic mouse model by crossing KP and miR-1 vascular-transgenic mice. The progeny of this breeding carried the two miR-1 overexpression constructs in addition to the floxed KRAS and P53 cassettes. miR-1 overexpression in these mice reduced the tumor burden by more than 85% (Figures 3E and 3F), confirming the critical role of miR-1 in the lung endothelium.

miR-1 Regulates Angiogenesis in the Lung

We next asked if miR-1 exerts a specific antiangiogenic effect or decreases tumor vascularity because of its antitumoral effects. We thus tested the effect of miR-1 in lung-specific VEGF transgenic mouse, which is a tumor-free model of lung angiogenesis (18). Intranasal treatment of these mice with a double-stranded miR-1 mimic decreased tracheal vascularity by 50% (Figure 4A). As described previously (13), this intranasal treatment increased miR-1 levels in the lung endothelium by more than 10 times without altering the VEGF levels (*see* Figures E4A and E4B). Vascular-specific overexpression of miR-1 through delivery of V-miR-1 vector had a similar effect and significantly reduced tracheal angiogenesis (Figure 4B), confirming the endothelial-specificity of the miR-1 effect.

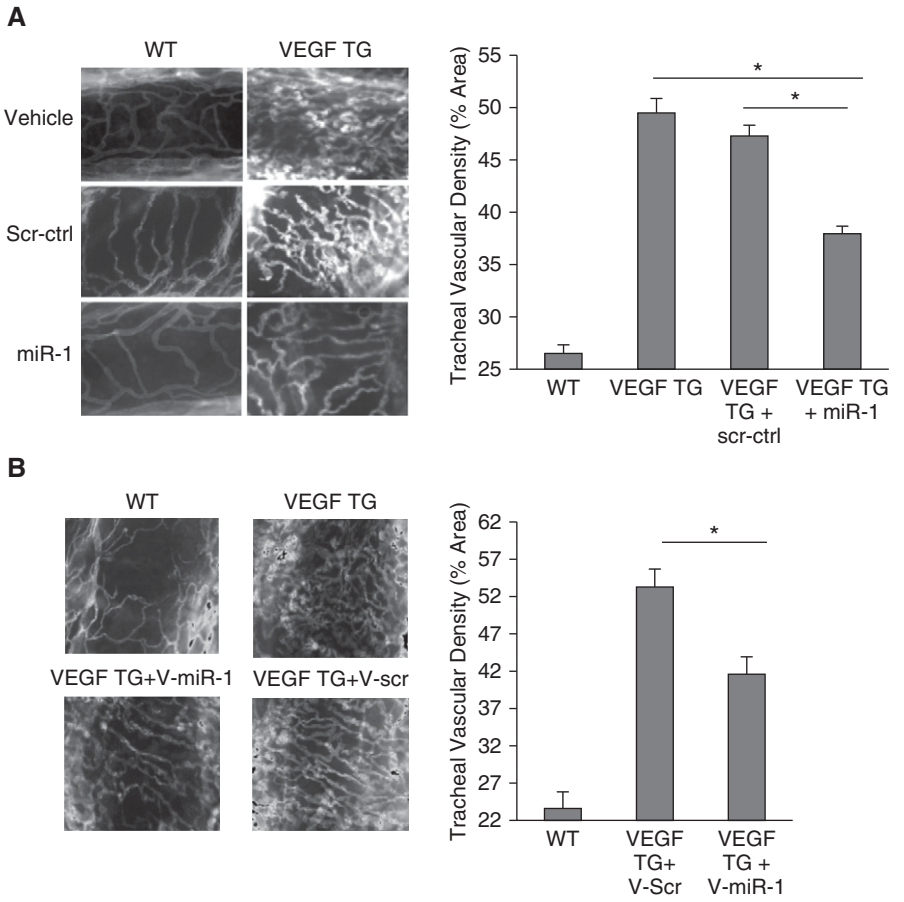

Figure 4. The effects of vascular-specific microRNA-1 (miR-1) on lung angiogenesis. (*A*) miR-1, scrambled control (scr-ctrl), or vehicle were delivered intranasally to vascular endothelial growth factor (VEGF) transgenic (VEGF TG) or wild-type (WT) mice 1 day after inducing the transgene. Lungs were harvested after 10 days. Tracheas were stained with anti-CD31 antibody. (*Left*) Representative images. (*Right*) Quantification of CD31-positive area (vascular density) expressed as a percentage of the whole area examined ($n \geq 8$ from four experiments; $^*P < 0.00001$). (*B*) Effect of vascular-specific miR-1 overexpression on tracheal vascular density. WT and VEGF TG mice received intranasal V-miR-1 or V-scr and VEGF transgene was induced by adding doxycycline to the drinking water. Tracheal vascular density was measured as described in *A*. (*Left*) Representative images. (*Right*) Results of quantification ($n \geq 6$ from three experiments; $^*P = 0.00970$). *Error bars* represent SEM. V-miR-1 = vascular-specific miR-1; V-scr = vascular-specific scrambled control.

miR-1 Regulates the Proliferation of Lung Endothelial Cells

To gain insight into the mechanism of the miR-1 antiangiogenic effect, we tested its effects on specific endothelial phenotypes of the MLECs. miR-1 transfection decreased VEGF-induced MLEC growth over a wide range of VEGF concentrations (Figures 5A and 5B) and reduced endothelial sprouting (Figure 5C), but did not affect survival or migration (*see* Figures E5A and E5B). We further examined this specific antiproliferative effect by testing the effect of miR-1 on *de novo* DNA synthesis (5-bromo-2'-deoxyuridine [BrdU], incorporation). As shown in Figure 5D, miR-1 transfection reduced BrdU incorporation by more than 30%.

miR-1 Regulates Proliferation and Extracellular Signal–regulated Protein Kinase Activation in Human Endothelial Cells

We next examined the role and regulation of miR-1 in human primary endothelial cells. We used HUVECs that are sensitive to VEGF and commonly used as an *in vitro* model of angiogenesis (19, 20). VEGF stimulation reduced miR-1 levels in HUVECs in a dose-dependent manner. Similar to our approach in MLECs, we verified the importance of this regulation by testing the effects of miR-1 alteration on VEGF-induced cell proliferation. Overexpression of miR-1 reduced the endothelial growth rate, whereas inhibition of miR-1 reduced this rate (Figures 6A and 6B). In complementary experiments, miR-1 reduced *de novo* DNA synthesis but did not alter apoptosis (Figures 6D and 6E). In signaling experiments (21), miR-1 specifically inhibited extracellular signal–regulated protein kinases (ERK) 1/2 phosphorylation at its peak (5 and 10 min) without affecting phosphoinositide 3-kinase (PI3 kinase), or JNK pathways (Figures 6F and 6G). We also observed that the relative phospho-P38/total P38 levels were higher at baseline in the miR-1–transfected cells, but did not find a consistent inhibitory effect on this axis.

miR-1 Is Regulated via the VEGFR2-PI3 Kinase Pathway

We next sought to determine the mechanism of miR-1 down-regulation. We have previously shown that lung miR-1 level is regulated through VEGF receptor 2 (VEGFR2) (13). We tested the role of four

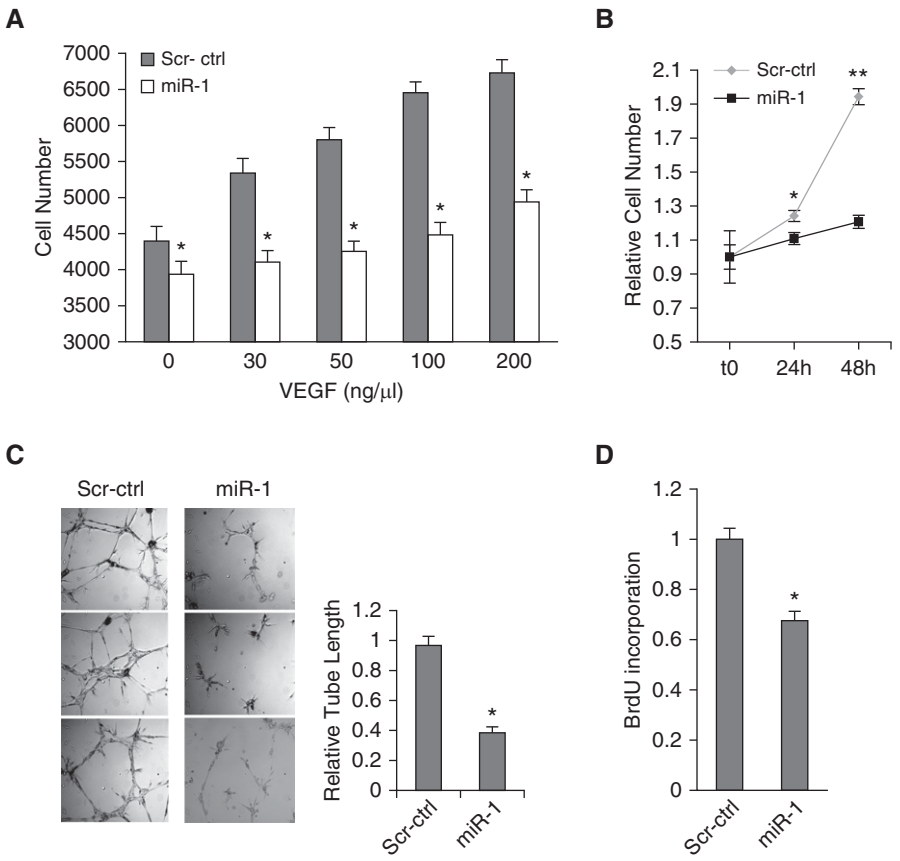

Figure 5. The effect of microRNA-1 on mouse lung endothelial cells (MLEC). (*A–D*) MLECs were transfected with double stranded miR-1 mimic (miR-1) or scrambled control RNA (Scr-ctrl) and stimulated with recombinant human vascular endothelial growth factor (VEGF)-A. (*A*) MLEC growth at 24 hours in response to various concentrations of VEGF was measured using WST-1 kit (Roche) (n = 6 from two experiments; $^*P < 0.05$). (*B*) MLEC growth in response to 50 ng/ml of VEGF at the indicated time points was measured as in *A* (*x-axis* shows time) (n = 24 from four experiments; $^*P < 0.01$, $^{**}P < 0.000001$). (*C*) Endothelial sprouting (capillary tube formation in matrigel). (*Left*) Representative images. (*Right*) Quantitation of the relative tube length (n = 9 from three experiments; $^*P < 0.005$). (*D*) Bromodeoxyuridine incorporation in response to VEGF was measured as an index of *de novo* DNA synthesis by ELISA (Roche) and values were normalized to the control reaction (n ⩾ 24 from six experiments; $^*P = 1.4 \times 10^{-6}$). *Error bars* represent SEM. BrdU = bromodeoxyuridine.

major VEGF signaling axes on miR-1 regulation by measuring the effects of their corresponding blockers on miR-1 levels. As shown in Figure 6H, among the ERK, P38, JNK, and PI3 kinase blockers, only PI3 kinase blockade inhibited VEGF-driven miR-1 down-regulation. Furthermore, blockade of Akt, a downstream effector of the PI3 kinase pathway, had a similar effect, confirming the role of the PI3 kinase in miR-1 down-regulation.

miR-1 Targets Thrombopoietin Receptor (Mpl) in the Lung Endothelium

Mpl is one of the miR-1 targets in the endothelium (13). We asked if miR-1 targets Mpl in the context of angiogenesis. VEGF overexpression increased Mpl levels in the lung and intranasal miR-1 delivery lowered Mpl levels in that context (Figures 7A and 7B). This inhibition corresponded to a 70% decrease of Mpl in the lung endothelial cells, suggesting that miR-1 is targeting Mpl in the endothelium. In accord with this finding, endothelial-specific overexpression of miR-1 also decreased lung endothelial Mpl levels (Figure 7C).

Mpl Regulates Angiogenesis in Mouse and Human Models

To determine the role of Mpl in angiogenesis, we first tested the effect of Mpl knockdown through siRNA delivery (13). Mpl knockdown reduced tracheal vascularity by approximately 50% (Figure 7D) and tumor angiogenesis by 30% (Figures 7E and 7F), closely resembling the inhibitory effects of miR-1 overexpression. Mpl knockdown in MLECs also mimicked miR-1 effects and significantly inhibited cellular growth and differentiation (Figure 7G; *see* Figure E6), and *de novo* DNA synthesis (Figure 7H). We next tested the role of Mpl in human primary endothelial cells. Consistent with its targeting by miR-1, Mpl knockdown decreased *de novo* DNA synthesis (Figure 8A) and ERK 1/2 activation in HUVECs (Figure 8B), and Mpl overexpression had the opposite effect in both assays (Figures 8C and 8D).

Discussion

Tumor progression is the result of a complex and multifaceted interaction between malignant cells and their microenvironment (2). However, recent efforts to "personalize" anticancer interventions have mostly focused on the tumor cells. We had previously shown that VEGF down-regulates miR-1 and that miR-1 regulates type 2 inflammation (13). In this manuscript we show that miR-1, a lung endothelial miRNA, is altered in NSCLC, and controls tumor progression and angiogenesis.

We found that miR-1 was significantly lower in NSCLC tumor samples and showed for the first time that tumor miR-1 levels have a direct correlation with overall survival of patients with NSCLC. We also observed a strong trend toward an inverse correlation between tumor miR-1 levels and the clinical stage ($P = 0.07$), which is consistent with association of miR-1 levels and survival. Statistical association between miR-1 levels and tumor progression has been previously reported for gastrointestinal and urinary cancers (22–25) and a recent study on 55 patients with NSCLC reported a correlation between miR-1 levels and venous metastasis (26). Another study on 33 squamous cell carcinoma samples reported lower miR-1 levels in tumors but no association with tumor progression (27). In our cohort, tumor miR-1 levels were lower than the cancer-free tissue in both adenocarcinoma and squamous cell carcinoma patients, but the correlation with survival was only observed in the adenocarcinoma subgroup, and later confirmed in a publicly available 542-patient cohort. We also observed lower miR-1 levels in an early lung adenocarcinoma cohort but could not

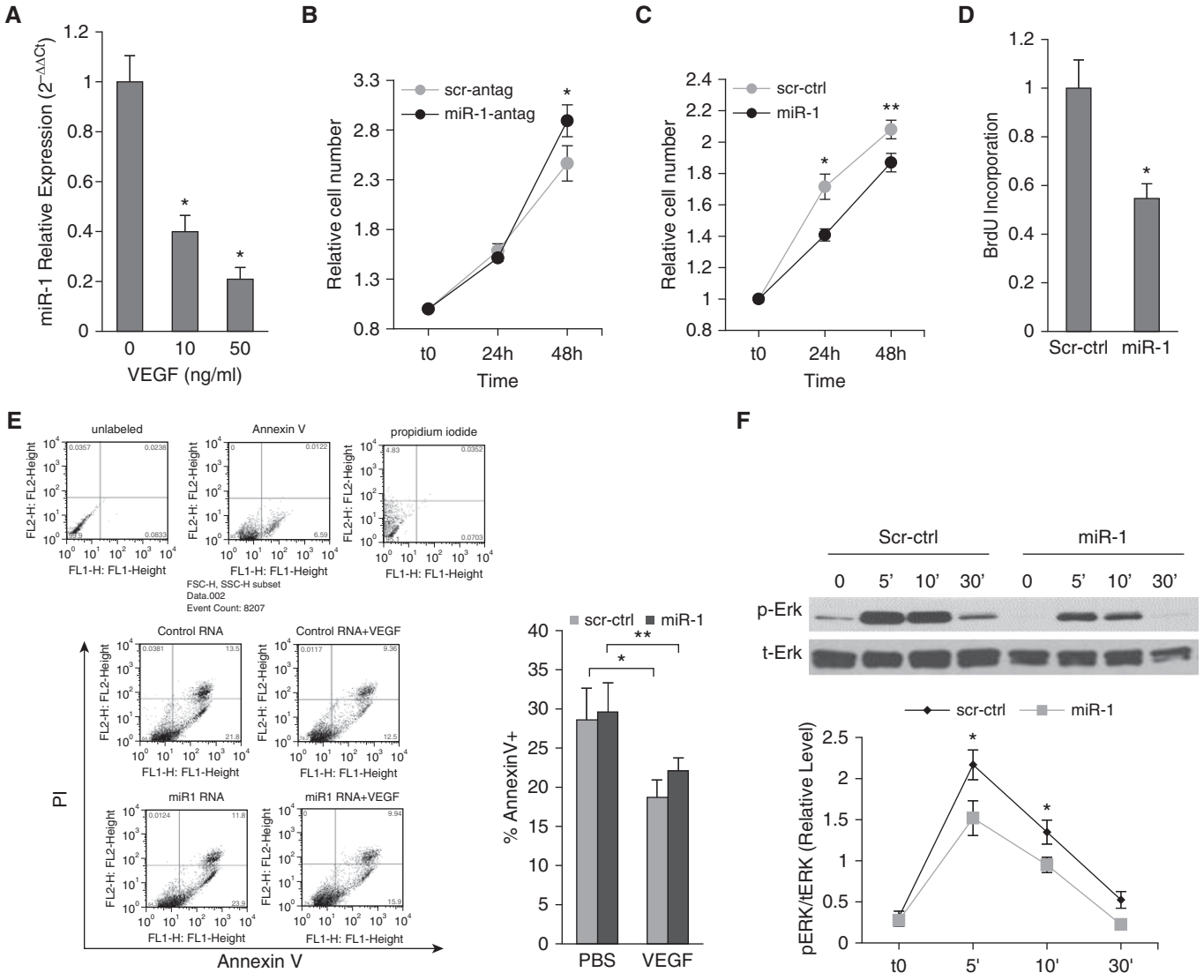

Figure 6. The role and regulation of microRNA-1 in human primary endothelial cells. (*A*) miR-1/18s levels were measured in human umbilical vein endothelial cells (HUVECs) stimulated with 10 ng or 50 ng/ml of recombinant human vascular endothelial growth factor (VEGF). Values were normalized to the mean of the control group and expressed as $2^{-\Delta\Delta Ct}$ ($n \geq 15$ from five experiments; $^{*}P < 0.0001$). (*B–E*) HUVECs were transfected with miR-1 antagomir (miR-1-antag), mature miR-1 double-stranded mimic (miR-1), or their respective scrambled controls (scr-antag, or scr-ctrl). HUVECs were then starved overnight and stimulated with VEGF (10 ng/ml). (*B*) The effects of miR-1-antag and its control on proliferation were measured and presented as in Figure 5A ($n = 12$ from two experiments; $^{*}P = 0.043$). (*C*) The effects of miR-1 and its control on proliferation were measured and presented as in Figure 5A ($n = 16$ from three experiments; $^{*}P = 0.00194$; $^{**}P = 0.0307$). (*D*) The effects of miR-1 and scr-ctrl on bromodeoxyuridine incorporation *(de novo* DNA synthesis) was measured and presented as in Figure 5D ($n = 20$ from four experiments; $^{*}P = 0.00123$). (*E*) The effect of miR-1 and scr-ctrl on cell death was analyzed by fluorescence-activated cell sorter analysis for Annexin V and propidium iodide (PI). (*Left*) Results of a typical fluorescence-activated cell sorter analysis experiments. (*Top*) Results of staining with each reagent in a representative experiment. (*Bottom left*) Representative dot plots for each experimental group. (*Bottom right*) Quantification of apoptotic cell fraction defined as a percentage of Annexin V–positive cells ($n \geq 6$ from two experiments; $^{*}P = 0.028$; $^{**}P = 0.047$). (*F* and *G*) HUVECs were transfected with miR-1 or scr-ctrl, starved overnight, and stimulated with VEGF. Reaction was stopped at 5, 10, or 30 minutes and cells were lysed. Phosphorylated and total extracellular signal–regulated protein kinase (ERK) (p-ERK and t-ERK, respectively) fractions were detected by Western blotting. (*F*) Representative immunoblot (*top*) and quantification of the activated ERK1/2 (p-ERK/t-ERK) (*bottom*) (*x-axis* shows time in minutes) ($n = 8$; $^{*}P < 0.04$). (*G*) Representative immunoblots for activated (phosphorylated, p-) and total (t-) P38 mitogen-activated protein kinase (P38K), phosphoinositide 3-kinase (PI3K), and c-jun N-terminal kinase (JNK). (*H*) HUVECs were starved, incubated with blockers, and stimulated with VEGF for 24 hours. miR-1 was measured as described in Figure 2 ($n \geq 10$ from five experiments; $^{*}P < 0.001$; $^{**}P < 1 \times 10^{-5}$). *Error bars* represent SEM. BrdU = bromodeoxyuridine; FSC = forward scatter; PBS = phosphate-buffered saline; SSC = side scatter.

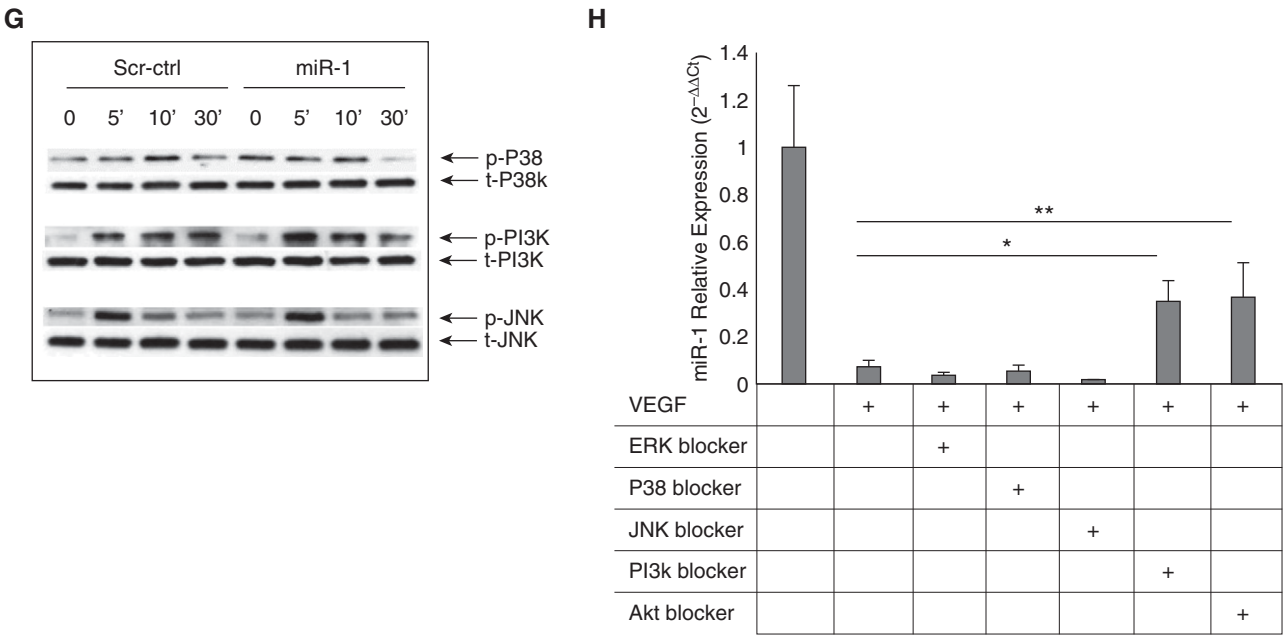

Figure 6. (Continued).

confirm the correlation with survival in that cohort because of inadequate data and short duration of follow-up. Even though these observations suggest a specificity for the miR-1 role in adenocarcinoma tumors, considering the smaller size of the squamous cell carcinoma subgroup within our cohort, we cannot confirm this specificity at this time.

We have found that PI3 kinase/Akt signaling pathway mediates miR-1 regulation in the endothelium. PI3 kinase pathway plays a significant role in initiation and propagation of tumors (28–32). The role of this pathway in the NSCLC microenvironment and its contribution to tumor resistance, and specifically tumor angiogenesis, have been demonstrated by various groups (33–37). Interestingly, a recent clinical study showed an inverse correlation between miR-1 and PI3 kinase in NSCLC tumors (26). Inhibition of miR-1 down-regulation through PI3 kinase blockade strongly suggests that PI3 kinase activation is the main mechanism regulating miR-1 levels in tumors.

Previous studies have shown that miR-1 regulates multiple aspects of the tumor cell behavior, such as proliferation (38, 39), motility (27, 40), apoptosis (41, 42), angiogenesis (43, 44), and glucose metabolism (45). Two recent studies suggested that miR-1 modulates the paracrine function of cancer-associated fibroblasts (46, 47), and one recent report showed that ectopic miR-1 modulates the extracellular vesicles released from glioblastoma tumor cells (48). However, demonstration of the endothelial-specific functions of miR-1 and mechanistic aspects of these effects are unique aspects of our study.

In vivo elucidation of the role of miRNAs in the tumor microenvironment has only been attempted in a few instances through delivery of nanocomplexes or engraftment of miRNA-transfected cells (49–52). These approaches are informative and therapeutically relevant but do not provide the clarity and stability of promoter-driven expression from a genomic locus. We, for the first time, used VE-cadherin promoter to overexpress miR-1 specifically in the tumor endothelium, confirmed the efficacy and specificity of miRNA expression with this method, and showed miR-1 antiangiogenic properties in various contexts.

We used both in LLC xenografts and *KRAS*/*P53* model in our experiments. *KRAS*/*P53* mouse is one of the most faithful models of NSCLC (53–56) and significant inhibition (>85%) of tumor growth in this model by endothelial-specific miR-1 demonstrates the critical role of miR-1 in the tumor endothelium. As a candidate mechanism for this role, we tested the effect of miR-1 on angiogenesis. miRNAs have differential effects on endothelial behavior (57, 58). miR-126 and miR-132 stimulate angiogenesis (49, 59), whereas miR-92a or miR-519c inhibit this process (60, 61). A previous study on zebrafish reported an antiangiogenic role for miR-1 and miR-206 (62). In line with this report, a few studies indicated that miR-1 targets VEGF in malignant cells (43, 44). Our findings in VEGF transgenic mice and in the *in vitro* VEGF supplementation experiments strongly suggest that the antiangiogenic effects of miR-1 can occur independent of its anti-VEGF properties. The VEGF transgene in our mouse model does not carry a 3′UTR, and its expression was not affected by miR-1 delivery (*see* Figure E3B). Furthermore, we could not find any statistical association between miR-1 and VEGF levels within our clinical cohorts (personal communication).

In mechanistic studies, alterations of the miR-1 levels inhibited endothelial cell growth and sprouting, without affecting cell death or migration. Cellular proliferation and differentiation require *de novo* DNA synthesis (3, 63), and miR-1 reduced this activity in a BrdU incorporation assay. Furthermore, miR-1 inhibited ERK1/2, which is one of the main signaling pathways downstream of VEGF mediating endothelial proliferation, sprouting, and *de novo* DNA synthesis (64–66). Inhibition of ERK by miR-1 is thus consistent with its antiangiogenic properties. However, it should be noted that direct proof for the functionality of this mechanism requires

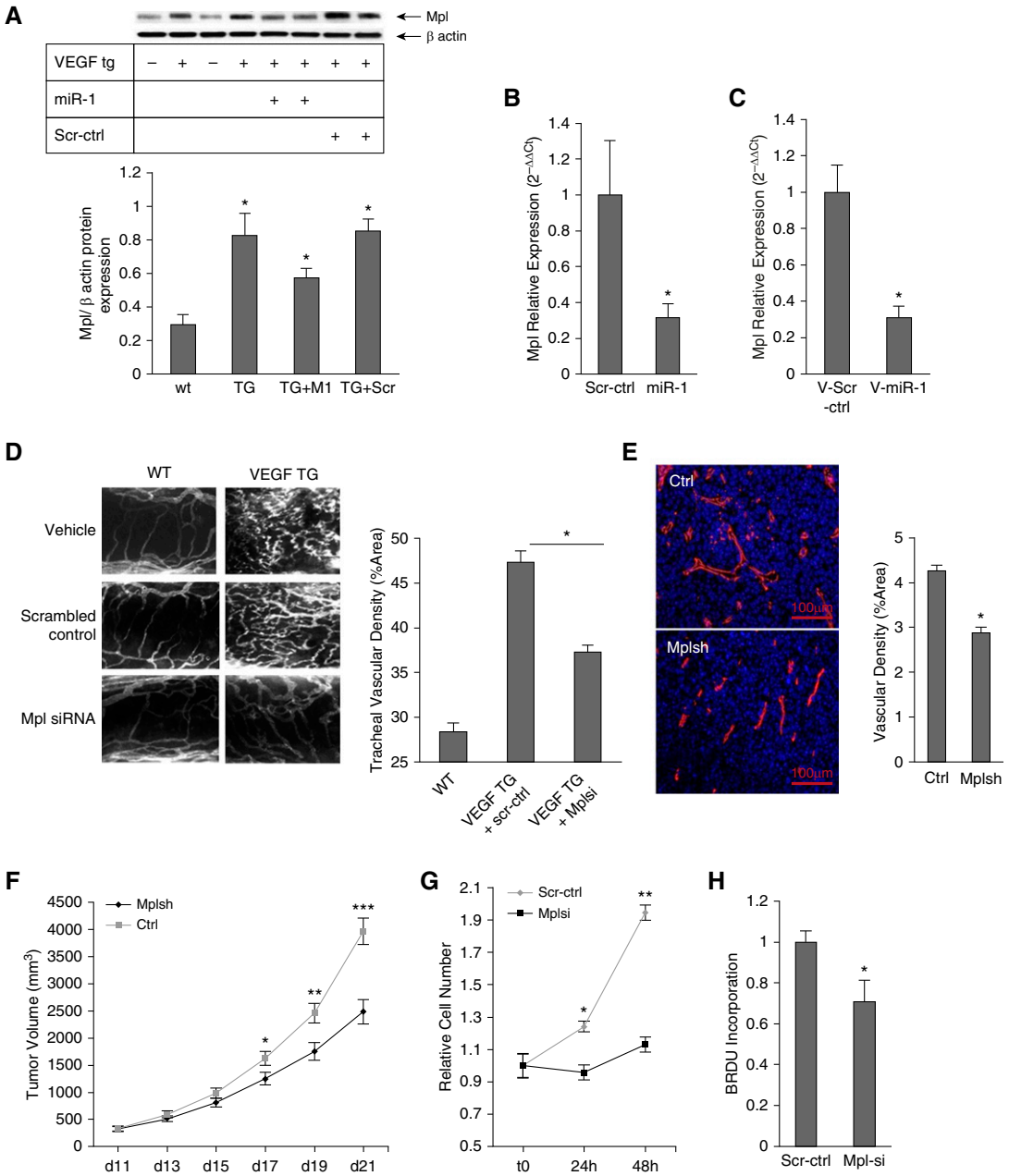

Figure 7. The role of myeloproliferative leukemia virus oncogene (Mpl) in angiogenesis and tumor growth. (*A*) Mpl expression was detected by Western blot analysis in the lungs of vascular endothelial growth factor (VEGF) transgenic (TG) mice (VEGF TG^{+}) and their wild-type (WT) littermates (WT/VEGF TG^{-}) that received double-stranded microRNA-1 (miR-1) or scrambled control (Scr-ctrl) RNA. (*Top*) Representative Western blot. (*Bottom*) Results of densitometric analysis (TG+M1 = VEGF TG + miR-1) (n = 3; **P* and ***P* < 0.05). (*B*) Mpl expression was measured by Taqman quantitative real-time polymerase chain reaction in lung endothelial cells isolated from mice that received intranasal miR-1 or Scr-ctrl-RNA. The graph shows Mpl/glyceraldehyde phosphate dehydrogenase levels normalized to the control group and expressed as $2^{-\Delta\Delta Ct}$ (n = 11 from four experiments; **P* < 0.03). (*C*) A similar measurement as shown in *B* on lung endothelial cells from mice that received vascular-specific lenti-miR-1 (V-miR-1) or control (V-Scr-ctrl). The graph shows Mpl/glyceraldehyde phosphate dehydrogenase levels normalized to the control group and expressed as $2^{-\Delta\Delta Ct}$ (n = 8, from two experiments; **P* < 0.002). (*D*) VEGF-TG and -WT mice received small interfering RNA (siRNA) against Mpl (Mplsi) or Scr-ctrl. Tracheas were isolated and angiogenesis was assessed as described in Figure 4A. (*Left*) Representative images of tracheal vessels from WT and TG mice treated with vehicle (buffer), Mpl siRNA, or scrambled control RNA (n = 9 from three experiments; *P* < 0.0005). (*E*) Lewis lung carcinoma implants were injected with lentiviral vector containing Mpl short hairpin RNA (shRNA) (Mplsh) or the control vector (Ctrl). Tumors were harvested on Day 21 and vascularity assessed after staining with anti-CD31 antibody (n = 14 from two experiments; **P* = 0.004923). (*F*) Tumor sizes were measured at the indicated time points and volumes calculated as in Figure 2E (n = 17 from two experiments; **P* = 0.01606, ***P* = 0.00302, ****P* = 4.07 × 10^{-5}). (*G* and *H*) Mouse lung endothelial cells were transfected with Mplsi or Scr-ctrl and stimulated with VEGF (50 ng/ml). (*G*) Cell proliferation was measured as described in Figure 1D (n = 24 from four experiments; **P* < 0.01, ***P* < 0.00001). (*H*) BrdU incorporation was compared between the two groups (values were normalized to the control reaction, n = 20 from four experiments; **P* = 0.02). *Error bars* represent SEM. BrdU = bromodeoxyuridine.

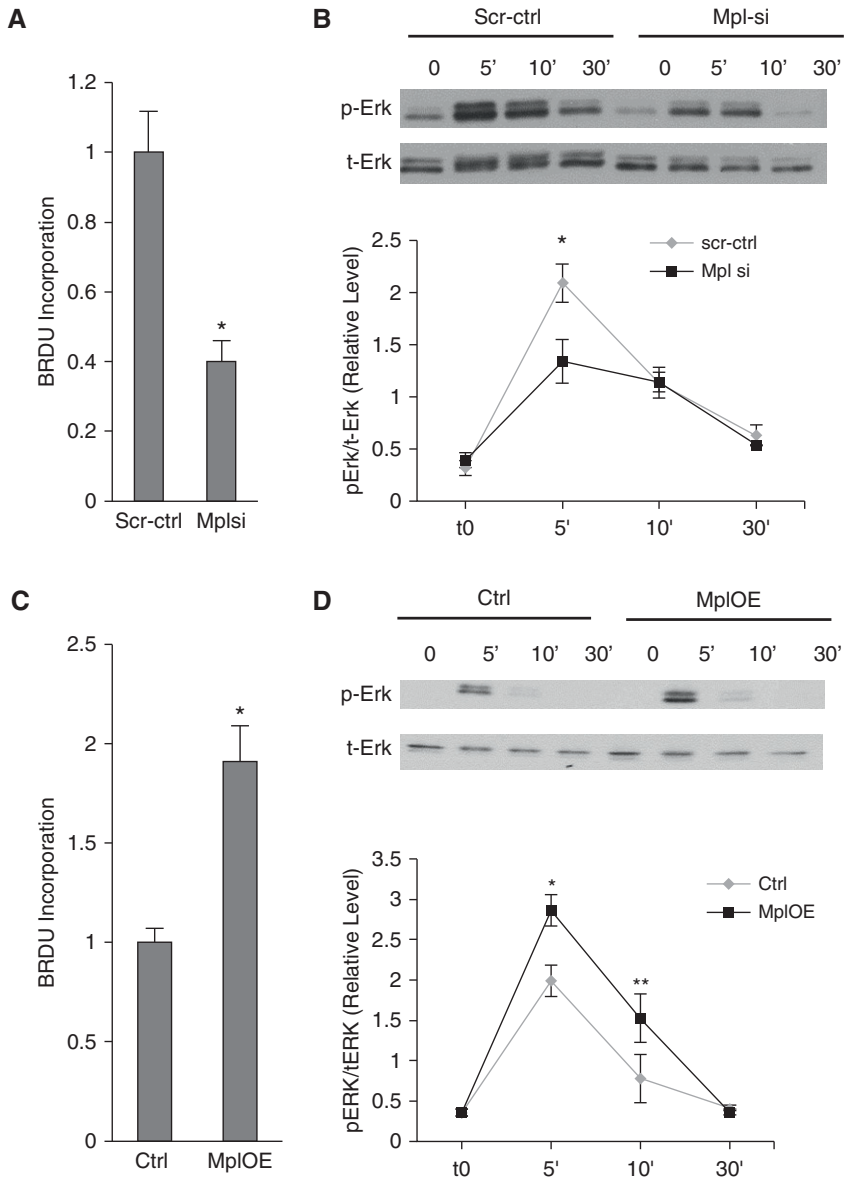

Figure 8. The role of myeloproliferative leukemia virus oncogene (Mpl) in human endothelial cells. (*A* and *B*) Human umbilical vein endothelial cells (HUVECs) were transfected with Mpl small interfering RNA (siRNA) (Mplsi) or scramble control RNA (scr-ctrl) and stimulated with vascular endothelial growth factor. (*A*) Bromodeoxyuridine (BrdU) incorporation in HUVEC was measured by ELISA and normalized to Scr-ctrl ($n \geq 5$ from four experiments; $^*P < 0.0005$). (*B*) Extracellular signal–regulated protein kinase (Erk) activation (phospho-Erk protein [pErk]/total Erk protein [tErk]) was measured as described in Figure 6F. (*Top*) Representative blot. (*Bottom*) Results of densitometric analysis (*x-axis* shows time in minutes) ($n = 6$ for each data point from three experiments; $^*P = 0.05$). (*C* and *D*) HUVECs were transfected with Mpl overexpression vector (MplOE) or control vector (Ctrl) and stimulated with vascular endothelial growth factor. (*C*) BrdU incorporation was measured and depicted as described in *C* ($n = 12$ from two experiments; $^*P < 0.0001$). (*D*) Erk activation was measured as described in *B* ($n = 6$ from six experiments; $^*P = 0.0026$; $^{**}P = 0.0344$). *Error bars* represent SEM.

in vivo measurement of ERK activity in the tumor endothelium. We also observed that miR-1–transfected endothelial cells show a higher level of P-38 activity at baseline (Figure 6G). P-38 activation leads to endothelial cell apoptosis (67, 68,) migration (69, 70), and inhibition of cell differentiation and ERK activation (67, 71). Even though activation of P-38 does not completely explain our observations, it is possible that this pathway contributes to the miR-1 antiangiogenic properties. It should also be noted that miR-1 antiproliferative effect is most probably only one of the endothelial phenotypes affected by miR-1, and other effects of miR-1 on endothelium await further inquiry.

We showed that miR-1 targets endothelial Mpl in the context of angiogenic activation and that Mpl knockdown mimicked miR-1 effects in the lung, tumor, and endothelial cells. Mpl is a type I cytokine receptor that mediates platelet production and hematopoietic stem cell maintenance (72) through activation of a number of downstream pathways, including STAT3 and 5 (73, 74), Shc-Grb2-SOS (75, 76), and Raf-1/MAP kinase (77, 78). Mpl is expressed in endothelial cells (79–81) and has been implicated in the angiogenic response within certain contexts (79, 82).

Our findings show for the first time that Mpl is one of the genes targeted by miR-1 in the lung microenvironment and suggest that Mpl mediates a significant portion of miR-1 inhibitory effects. Consistent with this idea, in preliminary experiments, overexpression of Mpl in the endothelium promoted tumor growth and angiogenesis, and reversed the inhibitory effects of miR-1 (personal communication). However, it should be noted that miRNAs target multiple genes and regulate cellular phenotypes through robust inhibition of multiple mediators (83), and that Mpl is most probably only one of the miR-1 mediators in endothelium. Further *in vivo*, such as Argonaute HITS-CLIP, will yield other novel miR-1 targets within the endothelium (84).

In this manuscript we used a variety of strategies to delineate the specific role and regulation of miR-1 in NSCLC tumors and the lung microenvironment. Our findings showed that miR-1 is a predictor of survival in patients with NSCLC, is regulated within the endothelium, and controls tumor growth and angiogenesis. These findings suggest that miR-1 may have clinical utility in the management and monitoring of patients on antiangiogenic therapy. ■

Author disclosures are available with the text of this article at www.atsjournals.org.

Acknowledgment: The authors thank Daniel J. Boffa (Yale Section of Thoracic Surgery) for his support and for providing tissues for our studies, and Maria Haslip (Yale Pulmonary and Critical Care Section) for her help with cellular apoptosis studies.

References

1. Cao Y, Arbiser J, D'Amato RJ, D'Amore PA, Ingber DE, Kerbel R, Klagsbrun M, Lim S, Moses MA, Zetter B, *et al*. Forty-year journey of angiogenesis translational research. *Sci Transl Med* 2011;3:114rv3.
2. Quail DF, Joyce JA. Microenvironmental regulation of tumor progression and metastasis. *Nat Med* 2013;19:1423–1437.
3. Dudley AC. Tumor endothelial cells. *Cold Spring Harb Perspect Med* 2012;2:a006536.
4. Jain RK. Antiangiogenesis strategies revisited: from starving tumors to alleviating hypoxia. *Cancer Cell* 2014;26:605–622.
5. Bartel DP. MicroRNAs: target recognition and regulatory functions. *Cell* 2009;136:215–233.
6. Lim LP, Lau NC, Garrett-Engele P, Grimson A, Schelter JM, Castle J, Bartel DP, Linsley PS, Johnson JM. Microarray analysis shows that some microRNAs downregulate large numbers of target mRNAs. *Nature* 2005;433:769–773.
7. Thum T, Gross C, Fiedler J, Fischer T, Kissler S, Bussen M, Galuppo P, Just S, Rottbauer W, Frantz S, *et al*. MicroRNA-21 contributes to myocardial disease by stimulating MAP kinase signalling in fibroblasts. *Nature* 2008;456:980–984.
8. Tay Y, Rinn J, Pandolfi PP. The multilayered complexity of ceRNA crosstalk and competition. *Nature* 2014;505:344–352.
9. Ameres SL, Zamore PD. Diversifying microRNA sequence and function. *Nat Rev Mol Cell Biol* 2013;14:475–488.
10. Pasquinelli AE. MicroRNAs and their targets: recognition, regulation and an emerging reciprocal relationship. *Nat Rev Genet* 2012;13:271–282.
11. Lu J, Getz G, Miska EA, Alvarez-Saavedra E, Lamb J, Peck D, Sweet-Cordero A, Ebert BL, Mak RH, Ferrando AA, *et al*. MicroRNA expression profiles classify human cancers. *Nature* 2005;435: 834–838.
12. Adams BD, Kasinski AL, Slack FJ. Aberrant regulation and function of microRNAs in cancer. *Curr Biol* 2014;24:R762–R776.
13. Takyar S, Vasavada H, Zhang JG, Ahangari F, Niu N, Liu Q, Lee CG, Cohn L, Elias JA. VEGF controls lung Th2 inflammation via the miR-1-Mpl (myeloproliferative leukemia virus oncogene)-P-selectin axis. *J Exp Med* 2013;210:1993–2010.
14. Lee CG, Link H, Baluk P, Homer RJ, Chapoval S, Bhandari V, Kang MJ, Cohn L, Kim YK, McDonald DM, *et al*. Vascular endothelial growth factor (VEGF) induces remodeling and enhances TH2-mediated sensitization and inflammation in the lung. *Nat Med* 2004;10: 1095–1103.
15. DuPage M, Dooley AL, Jacks T. Conditional mouse lung cancer models using adenoviral or lentiviral delivery of Cre recombinase. *Nat Protoc* 2009;4:1064–1072.
16. Takyar S, Zhang Y, Haslip M, Jin L, Shan P, Zhang X, Lee PJ. An endothelial TLR4-VEGFR2 pathway mediates lung protection against oxidant-induced injury. *FASEB J* 2016;30:1317–1327.
17. Kim DW, Uetsuki T, Kaziro Y, Yamaguchi N, Sugano S. Use of the human elongation factor 1 alpha promoter as a versatile and efficient expression system. *Gene* 1990;91:217–223.
18. Baluk P, Lee CG, Link H, Ator E, Haskell A, Elias JA, McDonald DM. Regulated angiogenesis and vascular regression in mice overexpressing vascular endothelial growth factor in airways. *Am J Pathol* 2004;165:1071–1085.
19. Wu LW, Mayo LD, Dunbar JD, Kessler KM, Ozes ON, Warren RS, Donner DB. VRAP is an adaptor protein that binds KDR, a receptor for vascular endothelial cell growth factor. *J Biol Chem* 2000;275:6059–6062.
20. Eubank TD, Galloway M, Montague CM, Waldman WJ, Marsh CB. M-CSF induces vascular endothelial growth factor production and angiogenic activity from human monocytes. *J Immunol* 2003;171: 2637–2643.
21. Claesson-Welsh L, Welsh M. VEGFA and tumour angiogenesis. *J Intern Med* 2013;273:114–127.
22. Xiao H, Zeng J, Li H, Chen K, Yu G, Hu J, Tang K, Zhou H, Huang Q, Li A, *et al*. MiR-1 downregulation correlates with poor survival in clear cell renal cell carcinoma where it interferes with cell cycle regulation and metastasis. *Oncotarget* 2015;6:13201–13215.
23. Yao L, Zhang Y, Zhu Q, Li X, Zhu S, Gong L, Han X, Lan M, Li S, Zhang W, *et al*. Downregulation of microRNA-1 in esophageal squamous cell carcinoma correlates with an advanced clinical stage and its overexpression inhibits cell migration and invasion. *Int J Mol Med* 2015;35:1033–1041.
24. Goto Y, Kurozumi A, Enokida H, Ichikawa T, Seki N. Functional significance of aberrantly expressed microRNAs in prostate cancer. *Int J Urol* 2015;22:242–252.
25. Datta J, Kutay H, Nasser MW, Nuovo GJ, Wang B, Majumder S, Liu CG, Volinia S, Croce CM, Schmittgen TD, *et al*. Methylation mediated silencing of MicroRNA-1 gene and its role in hepatocellular carcinogenesis. *Cancer Res* 2008;68:5049–5058.
26. Zhao Q, Zhang B, Shao Y, Chen L, Wang X, Zhang Z, Shu Y, Guo R. Correlation between the expression levels of miR-1 and PIK3CA in non-small-cell lung cancer and their relationship with clinical characteristics and prognosis. *Future Oncol* 2014;10:49–57.
27. Mataki H, Enokida H, Chiyomaru T, Mizuno K, Matsushita R, Goto Y, Nishikawa R, Higashimoto I, Samukawa T, Nakagawa M, *et al*. Downregulation of the microRNA-1/133a cluster enhances cancer cell migration and invasion in lung-squamous cell carcinoma via regulation of Coronin1C. *J Hum Genet* 2015;60:53–61.
28. Engelman JA. The role of phosphoinositide 3-kinase pathway inhibitors in the treatment of lung cancer. *Clin Cancer Res* 2007;13:s4637–s4640.
29. Solomon B, Pearson RB. Class IA phosphatidylinositol 3-kinase signaling in non-small cell lung cancer. *J Thorac Oncol* 2009;4:787–791.
30. Wong KK, Engelman JA, Cantley LC. Targeting the PI3K signaling pathway in cancer. *Curr Opin Genet Dev* 2010;20:87–90.
31. Engelman JA. Targeting PI3K signalling in cancer: opportunities, challenges and limitations. *Nat Rev Cancer* 2009;9:550–562.
32. Vivanco I, Sawyers CL. The phosphatidylinositol 3-Kinase AKT pathway in human cancer. *Nat Rev Cancer* 2002;2:489–501.
33. Prevo R, Deutsch E, Sampson O, Diplexcito J, Cengel K, Harper J, O'Neill P, McKenna WG, Patel S, Bernhard EJ. Class I PI3 kinase inhibition by the pyridinylfuranopyrimidine inhibitor PI-103 enhances tumor radiosensitivity. *Cancer Res* 2008;68:5915–5923.
34. Qayum N, Muschel RJ, Im JH, Balathasan L, Koch CJ, Patel S, McKenna WG, Bernhard EJ. Tumor vascular changes mediated by inhibition of oncogenic signaling. *Cancer Res* 2009;69:6347–6354.
35. Gupta AK, Cerniglia GJ, Mick R, McKenna WG, Muschel RJ. HIV protease inhibitors block Akt signaling and radiosensitize tumor cells both in vitro and in vivo. *Cancer Res* 2005;65:8256–8265.
36. Pore N, Gupta AK, Cerniglia GJ, Jiang Z, Bernhard EJ, Evans SM, Koch CJ, Hahn SM, Maity A. Nelfinavir down-regulates hypoxia-inducible factor 1alpha and VEGF expression and increases tumor oxygenation: implications for radiotherapy. *Cancer Res* 2006;66:9252–9259.
37. Graves EE, Maity A, Le QT. The tumor microenvironment in non-small-cell lung cancer. *Semin Radiat Oncol* 2010;20:156–163.
38. Stope MB, Stender C, Schubert T, Peters S, Weiss M, Ziegler P, Zimmermann U, Walther R, Burchardt M. Heat-shock protein HSPB1 attenuates microRNA miR-1 expression thereby restoring oncogenic pathways in prostate cancer cells. *Anticancer Res* 2014;34:3475–3480.
39. Reid JF, Sokolova V, Zoni E, Lampis A, Pizzamiglio S, Bertan C, Zanutto S, Perrone F, Camerini T, Gallino G, *et al*. miRNA profiling in colorectal cancer highlights miR-1 involvement in MET-dependent proliferation. *Mol Cancer Res* 2012;10:504–515.
40. Xu L, Zhang Y, Wang H, Zhang G, Ding Y, Zhao L. Tumor suppressor miR-1 restrains epithelial-mesenchymal transition and metastasis of colorectal carcinoma via the MAPK and PI3K/AKT pathway. *J Transl Med* 2014;12:244.
41. Yamasaki T, Yoshino H, Enokida H, Hidaka H, Chiyomaru T, Nohata N, Kinoshita T, Fuse M, Seki N, Nakagawa M. Novel molecular targets regulated by tumor suppressors microRNA-1 and microRNA-133a in bladder cancer. *Int J Oncol* 2012;40:1821–1830.
42. Nohata N, Hanazawa T, Kikkawa N, Sakurai D, Sasaki K, Chiyomaru T, Kawakami K, Yoshino H, Enokida H, Nakagawa M, *et al*. Identification of novel molecular targets regulated by tumor suppressive miR-1/miR-133a in maxillary sinus squamous cell carcinoma. *Int J Oncol* 2011;39:1099–1107.
43. Li SL, Ma XH, Ji JF, Li H, Liu W, Lu FZ, Wu ST, Zhang Y. miR-1 association with cell proliferation inhibition and apoptosis in vestibular schwannoma by targeting VEGFA. *Genet Mol Res* 2016;15:gmr15048923.
44. Niu J, Sun Y, Guo Q, Niu D, Liu B. miR-1 inhibits cell growth, migration, and invasion by targeting VEGFA in osteosarcoma cells. *Dis Markers* 2016;2016:7068986.

45. Singh A, Happel C, Manna SK, Acquaah-Mensah G, Carrerero J, Kumar S, Nasipuri P, Krausz KW, Wakabayashi N, Dewi R, *et al*. Transcription factor NRF2 regulates miR-1 and miR-206 to drive tumorigenesis. *J Clin Invest* 2013;123:2921–2934.
46. Li J, Guan J, Long X, Wang Y, Xiang X. mir-1-mediated paracrine effect of cancer-associated fibroblasts on lung cancer cell proliferation and chemoresistance. *Oncol Rep* 2016;35:3523–3531.
47. Shen H, Yu X, Yang F, Zhang Z, Shen J, Sun J, Choksi S, Jitkaew S, Shu Y. Reprogramming of normal fibroblasts into cancer-associated fibroblasts by miRNAs-mediated CCL2/VEGFA signaling. *PLoS Genet* 2016;12:e1006244.
48. Bronisz A, Wang Y, Nowicki MO, Peruzzi P, Ansari K, Ogawa D, Balaj L, De Rienzo G, Mineo M, Nakano I, *et al*. Extracellular vesicles modulate the glioblastoma microenvironment via a tumor suppression signaling network directed by miR-1. *Cancer Res* 2014; 74:738–750.
49. Anand S, Majeti BK, Acevedo LM, Murphy EA, Mukthavaram R, Scheppke L, Huang M, Shields DJ, Lindquist JN, Lapinski PE, *et al*. MicroRNA-132-mediated loss of p120RasGAP activates the endothelium to facilitate pathological angiogenesis. *Nat Med* 2010; 16:909–914.
50. Cubillos-Ruiz JR, Baird JR, Tesone AJ, Rutkowski MR, Scarlett UK, Camposeco-Jacobs AL, Anadon-Arnillas J, Harwood NM, Korc M, Fiering SN, *et al*. Reprogramming tumor-associated dendritic cells in vivo using miRNA mimetics triggers protective immunity against ovarian cancer. *Cancer Res* 2012;72:1683–1693.
51. Wei J, Wang F, Kong LY, Xu S, Doucette T, Ferguson SD, Yang Y, McEnery K, Jethwa K, Gjyshi O, *et al*. miR-124 inhibits STAT3 signaling to enhance T cell-mediated immune clearance of glioma. *Cancer Res* 2013;73:3913–3926.
52. Huang TH, Chu TY. Repression of miR-126 and upregulation of adrenomedullin in the stromal endothelium by cancer-stromal cross talks confers angiogenesis of cervical cancer. *Oncogene* 2014;33:3636–3647.
53. Edmonds MD, Boyd KL, Moyo T, Mitra R, Duszynski R, Arrate MP, Chen X, Zhao Z, Blackwell TS, Andl T, *et al*. MicroRNA-31 initiates lung tumorigenesis and promotes mutant KRAS-driven lung cancer. *J Clin Invest* 2016;126:349–364.
54. Ungewiss C, Rizvi ZH, Roybal JD, Peng DH, Gold KA, Shin DH, Creighton CJ, Gibbons DL. The microRNA-200/Zeb1 axis regulates ECM-dependent β1-integrin/FAK signaling, cancer cell invasion and metastasis through CRKL. *Sci Rep* 2016;6:18652.
55. Wang J, Hu K, Guo J, Cheng F, Lv J, Jiang W, Lu W, Liu J, Pang X, Liu M. Suppression of KRas-mutant cancer through the combined inhibition of KRAS with PLK1 and ROCK. *Nat Commun* 2016;7:11363.
56. McFadden DG, Politi K, Bhutkar A, Chen FK, Song X, Pirun M, Santiago PM, Kim-Kiselak C, Platt JT, Lee E, *et al*. Mutational landscape of EGFR-, MYC-, and Kras-driven genetically engineered mouse models of lung adenocarcinoma. *Proc Natl Acad Sci USA* 2016;113: E6409–E6417.
57. Wang S, Olson EN. AngiomiRs: key regulators of angiogenesis. *Curr Opin Genet Dev* 2009;19:205–211.
58. Weis SM, Cheresh DA. Tumor angiogenesis: molecular pathways and therapeutic targets. *Nat Med* 2011;17:1359–1370.
59. Wang S, Aurora AB, Johnson BA, Qi X, McAnally J, Hill JA, Richardson JA, Bassel-Duby R, Olson EN. The endothelial-specific microRNA miR-126 governs vascular integrity and angiogenesis. *Dev Cell* 2008; 15:261–271.
60. Bonauer A, Carmona G, Iwasaki M, Mione M, Koyanagi M, Fischer A, Burchfield J, Fox H, Doebele C, Ohtani K, *et al*. MicroRNA-92a controls angiogenesis and functional recovery of ischemic tissues in mice. *Science* 2009;324:1710–1713.
61. Cha ST, Chen PS, Johansson G, Chu CY, Wang MY, Jeng YM, Yu SL, Chen JS, Chang KJ, Jee SH, *et al*. MicroRNA-519c suppresses hypoxia-inducible factor-1alpha expression and tumor angiogenesis. *Cancer Res* 2010;70:2675–2685.
62. Stahlhut C, Suárez Y, Lu J, Mishima Y, Giraldez AJ. miR-1 and miR-206 regulate angiogenesis by modulating VegfA expression in zebrafish. *Development* 2012;139:4356–4364.
63. Cantelmo AR, Brajic A, Carmeliet P. Endothelial metabolism driving angiogenesis: emerging concepts and principles. *Cancer J* 2015;21: 244–249.
64. Takahashi T, Yamaguchi S, Chida K, Shibuya M. A single autophosphorylation site on KDR/Flk-1 is essential for VEGF-A-dependent activation of PLC-gamma and DNA synthesis in vascular endothelial cells. *EMBO J* 2001;20:2768–2778.
65. Sheikh AQ, Taghian T, Hemingway B, Cho H, Kogan AB, Narmoneva DA. Regulation of endothelial MAPK/ERK signalling and capillary morphogenesis by low-amplitude electric field. J R Soc Interface 2013;10:20120548.
66. Xu J, Liu X, Jiang Y, Chu L, Hao H, Liua Z, Verfaillie C, Zweier J, Gupta K, Liu Z. MAPK/ERK signalling mediates VEGF-induced bone marrow stem cell differentiation into endothelial cell. *J Cell Mol Med* 2008;12:2395–2406.
67. Matsumoto T, Turesson I, Book M, Gerwins P, Claesson-Welsh L. p38 MAP kinase negatively regulates endothelial cell survival, proliferation, and differentiation in FGF-2-stimulated angiogenesis. *J Cell Biol* 2002;156:149–160.
68. Gratton JP, Morales-Ruiz M, Kureishi Y, Fulton D, Walsh K, Sessa WC. Akt down-regulation of p38 signaling provides a novel mechanism of vascular endothelial growth factor-mediated cytoprotection in endothelial cells. *J Biol Chem* 2001;276:30359–30365.
69. McMullen M, Keller R, Sussman M, Pumiglia K. Vascular endothelial growth factor-mediated activation of p38 is dependent upon Src and RAFTK/Pyk2. *Oncogene* 2004;23:1275–1282.
70. Rousseau S, Houle F, Landry J, Huot J. p38 MAP kinase activation by vascular endothelial growth factor mediates actin reorganization and cell migration in human endothelial cells. *Oncogene* 1997;15:2169–2177.
71. Issbrücker K, Marti HH, Hippenstiel S, Springmann G, Voswinckel R, Gaumann A, Breier G, Drexler HC, Suttorp N, Clauss M. p38 MAP kinase: a molecular switch between VEGF-induced angiogenesis and vascular hyperpermeability. *FASEB J* 2003;17:262–264.
72. Hitchcock IS, Kaushansky K. Thrombopoietin from beginning to end. *Br J Haematol* 2014;165:259–268.
73. Drachman JG, Kaushansky K. Dissecting the thrombopoietin receptor: functional elements of the Mpl cytoplasmic domain. *Proc Natl Acad Sci USA* 1997;94:2350–2355.
74. Socolovsky M, Fallon AE, Wang S, Brugnara C, Lodish HF. Fetal anemia and apoptosis of red cell progenitors in Stat5a-/-5b-/- mice: a direct role for Stat5 in Bcl-X(L) induction. *Cell* 1999;98:181–191.
75. Sasaki K, Odai H, Hanazono Y, Ueno H, Ogawa S, Langdon WY, Tanaka T, Miyagawa K, Mitani K, Yazaki Y, *et al*. TPO/c-mpl ligand induces tyrosine phosphorylation of multiple cellular proteins including proto-oncogene products, Vav and c-Cbl, and Ras signaling molecules. *Biochem Biophys Res Commun* 1995;216:338–347.
76. Hill RJ, Zozulya S, Lu YL, Hollenbach PW, Joyce-Shaikh B, Bogenberger J, Gishizky ML. Differentiation induced by the c-Mpl cytokine receptor is blocked by mutant Shc adaptor protein. *Cell Growth Differ* 1996;7:1125–1134.
77. Nagata Y, Todokoro K. Thrombopoietin induces activation of at least two distinct signaling pathways. *FEBS Lett* 1995;377:497–501.
78. Yamada M, Komatsu N, Okada K, Kato T, Miyazaki H, Miura Y. Thrombopoietin induces tyrosine phosphorylation and activation of mitogen-activated protein kinases in a human thrombopoietin-dependent cell line. *Biochem Biophys Res Commun* 1995;217:230–237.
79. Brizzi MF, Battaglia E, Montrucchio G, Dentelli P, Del Sorbo L, Garbarino G, Pegoraro L, Camussi G. Thrombopoietin stimulates endothelial cell motility and neoangiogenesis by a platelet-activating factor-dependent mechanism. *Circ Res* 1999;84:785–796.
80. Zhang J, Freyer D, Rung O, Im AR, Hoffmann O, Dame C. Inflammation stimulates thrombopoietin (Tpo) expression in rat brain-derived microvascular endothelial cells, but suppresses Tpo in astrocytes and microglia. *J Interferon Cytokine Res* 2010;30:465–469.
81. Cardier JE, Dempsey J. Thrombopoietin and its receptor, c-mpl, are constitutively expressed by mouse liver endothelial cells: evidence of thrombopoietin as a growth factor for liver endothelial cells. *Blood* 1998;91:923–929.
82. Amano H, Hackett NR, Rafii S, Crystal RG. Thrombopoietin gene transfer-mediated enhancement of angiogenic responses to acute ischemia. *Circ Res* 2005;97:337–345.
83. Ebert MS, Sharp PA. Roles for microRNAs in conferring robustness to biological processes. *Cell* 2012;149:515–524.
84. Chi SW, Zang JB, Mele A, Darnell RB. Argonaute HITS-CLIP decodes microRNA-mRNA interaction maps. *Nature* 2009;460:479–486.